Supplementary Information (SI) for Journal of Materials Chemistry A.

Atomic Layered NiO/Phosphorus-Doped MnO_2 P-N Junctions: A Pathway to High-Performance Supercapattery Devices

Sangeeta Adhikari[a,b,1], *Gi-Hyeok Noh*[a,1], *Amarnath T. Sivagurunathan*[a], *Do-Heyoung Kim*[a,*]

[a]*School of Chemical Engineering, Chonnam National University, 77, Yongbong-ro, Buk-gu, Gwangju, 61186, Republic of Korea*

[b]*Catalyst Research Institute, Chonnam National University, 77, Yongbong-ro, Buk-gu, Gwangju, 61186, Republic of Korea*

[1]*Equal Contribution*

Supporting Information

*Corresponding author

Prof. Do-Heyoung Kim, Email: kdhh@chonnam.ac.kr

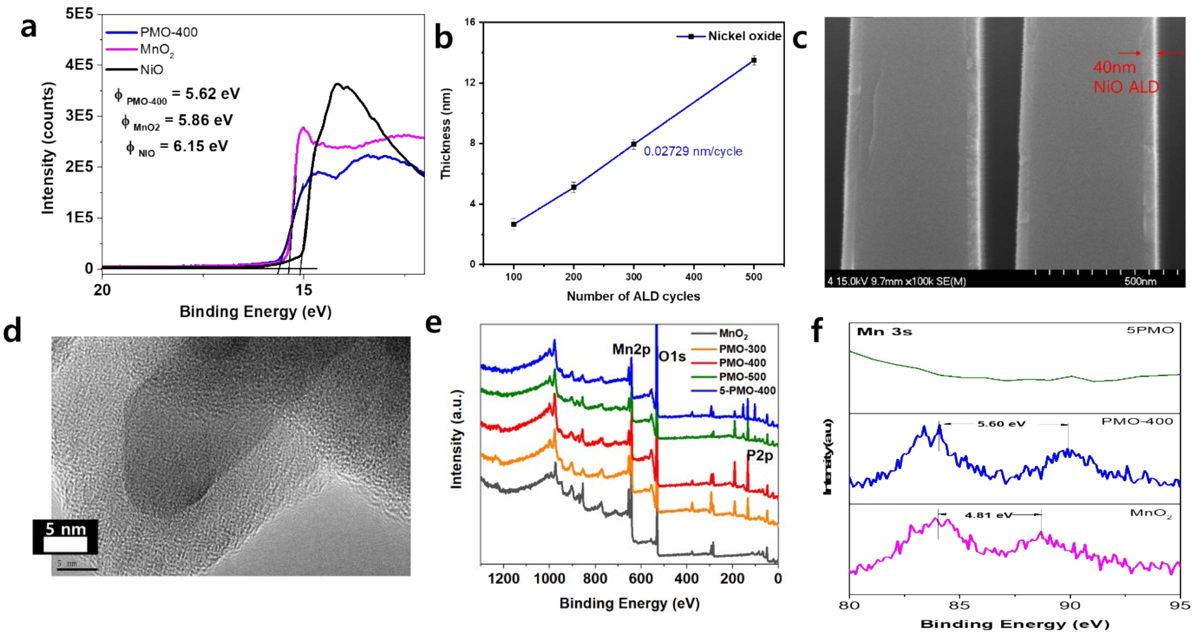

Figure S1. (a) UPS data with corresponding work function for NiO, MnO_2 and PMO-400 ; (b) Linearity process for ALD NiO; (c) 40 nm NiO deposited on patterned silicon wafer; (d) HRTEM image of 7.5 nm NiO deposited PMO-400 electrode; (e) XPS Survey scan of MnO_2, PMO-300, PMO-400, PMO-500 and 5PMO; and (f) Mn 3s XPS spectra for the prepared MnO_2, PMO-400 and 5PMO electrodes.

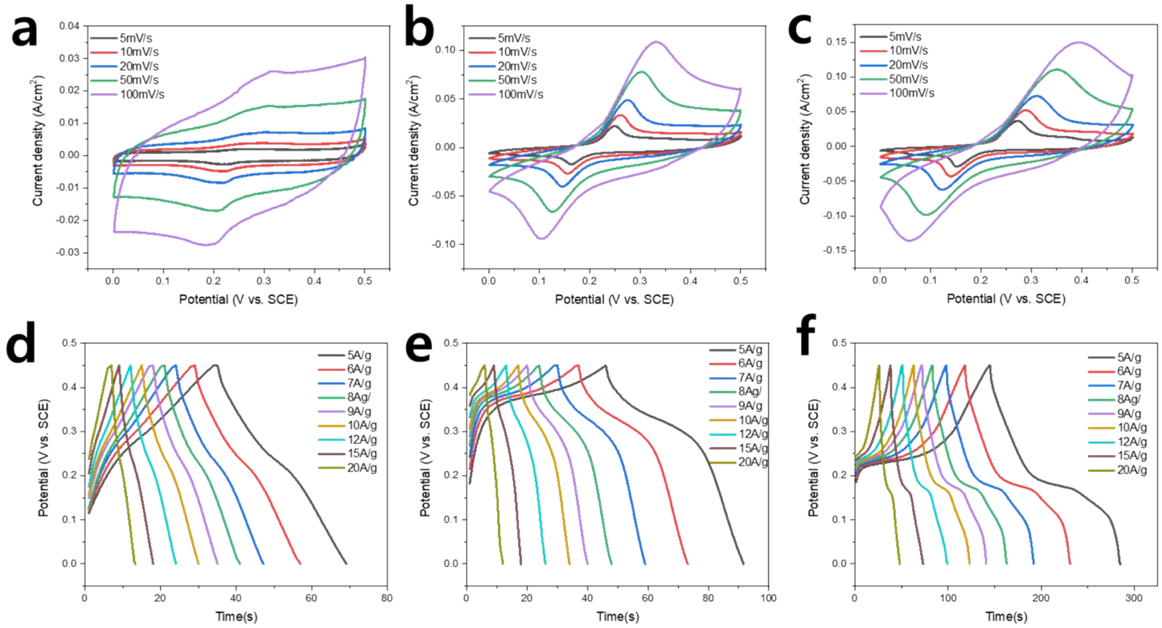

Figure S2. CV and GCD curves of (a, d) MnO_2, (b, e) PMO-300, and (c, f) PMO-500.

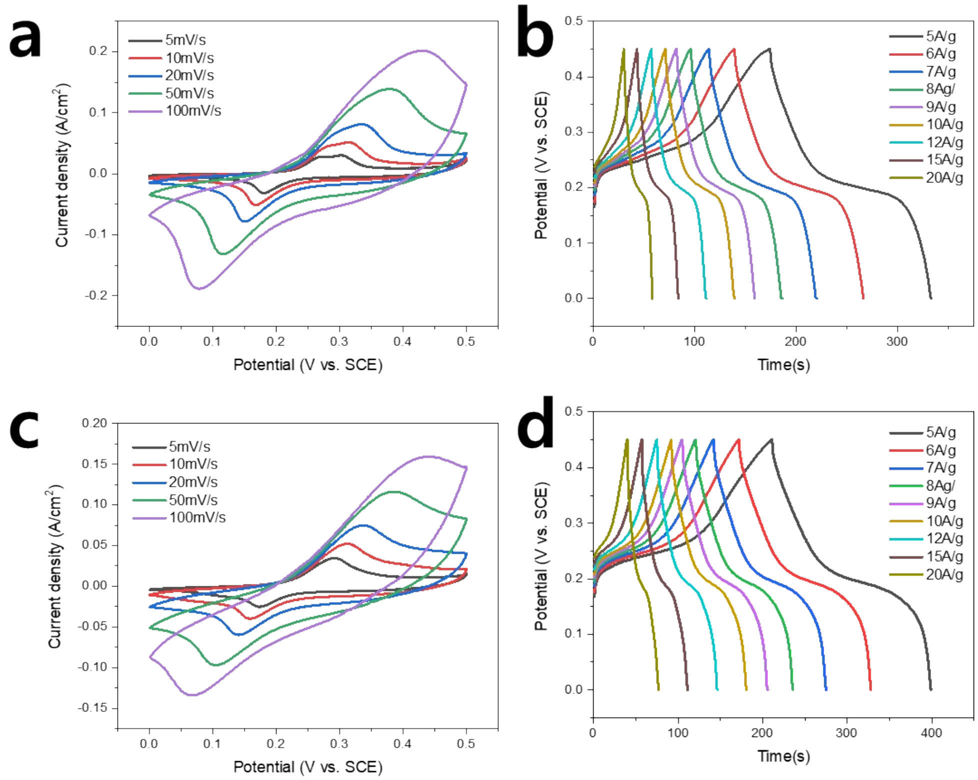

Figure S3. CV and GCD curves of (a, b) 2.5PMO, and (c, d) 7.5PMO electrodes.

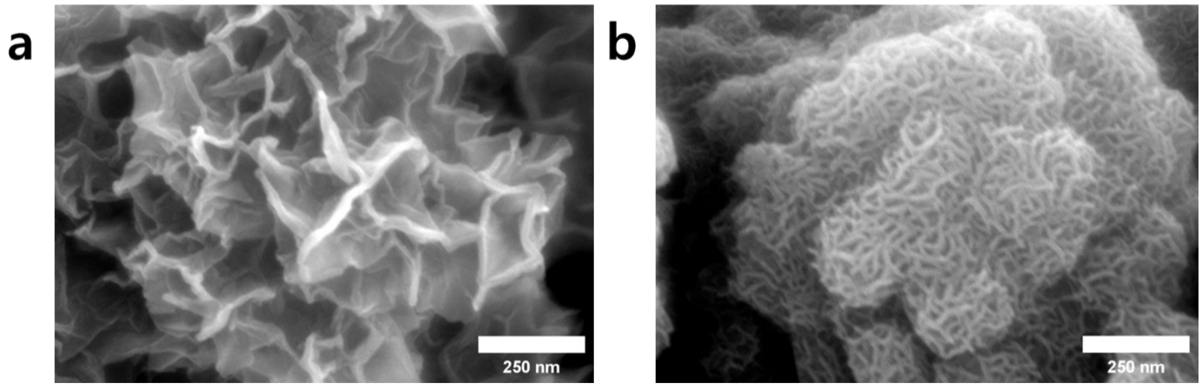

Figure S4. FESEM images of (a) PMO-400 and (b) 5PMO after 20000 charge-discharge cycles.

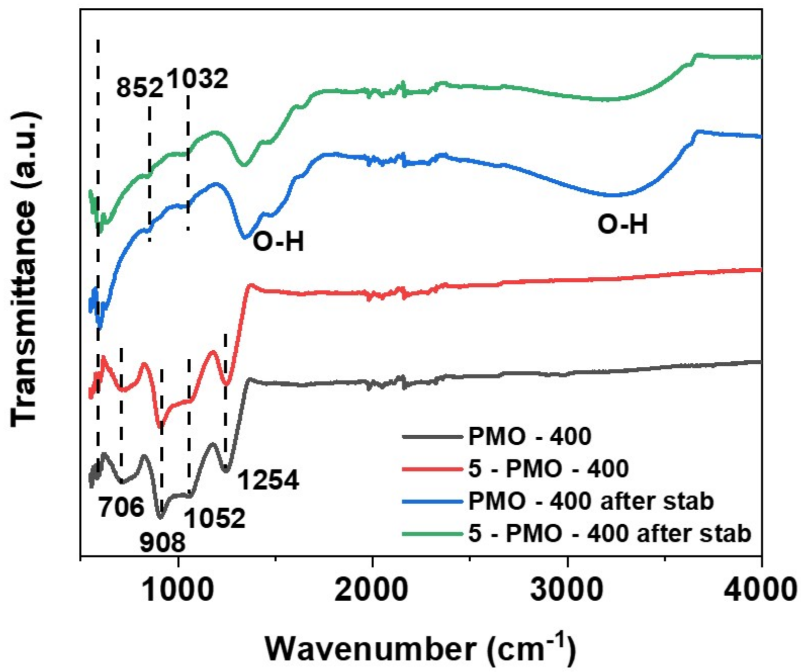

Figure S5. Comparative FTIR spectra for pristine and after 20000 cycles of PMO-400, and 5PMO electrodes.

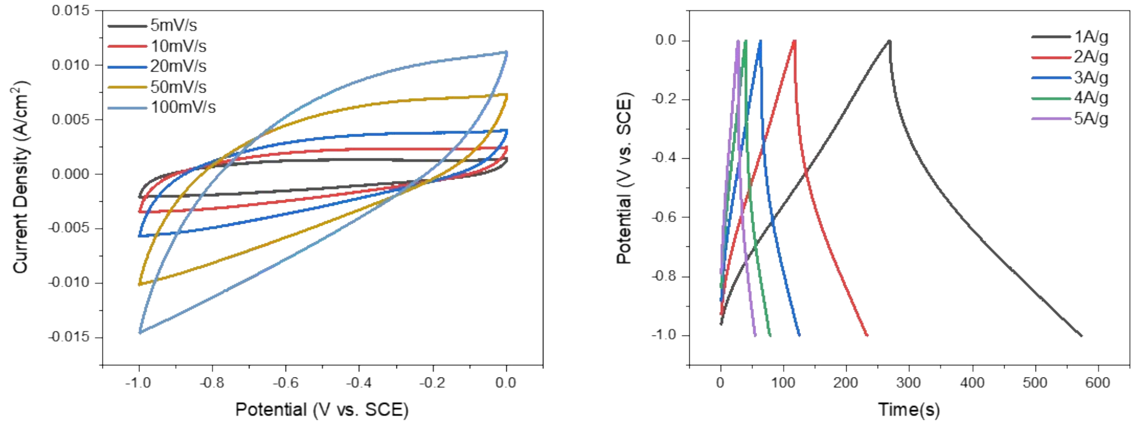

Figure S6. CV and GCD curves of rGO on Ni-foam.

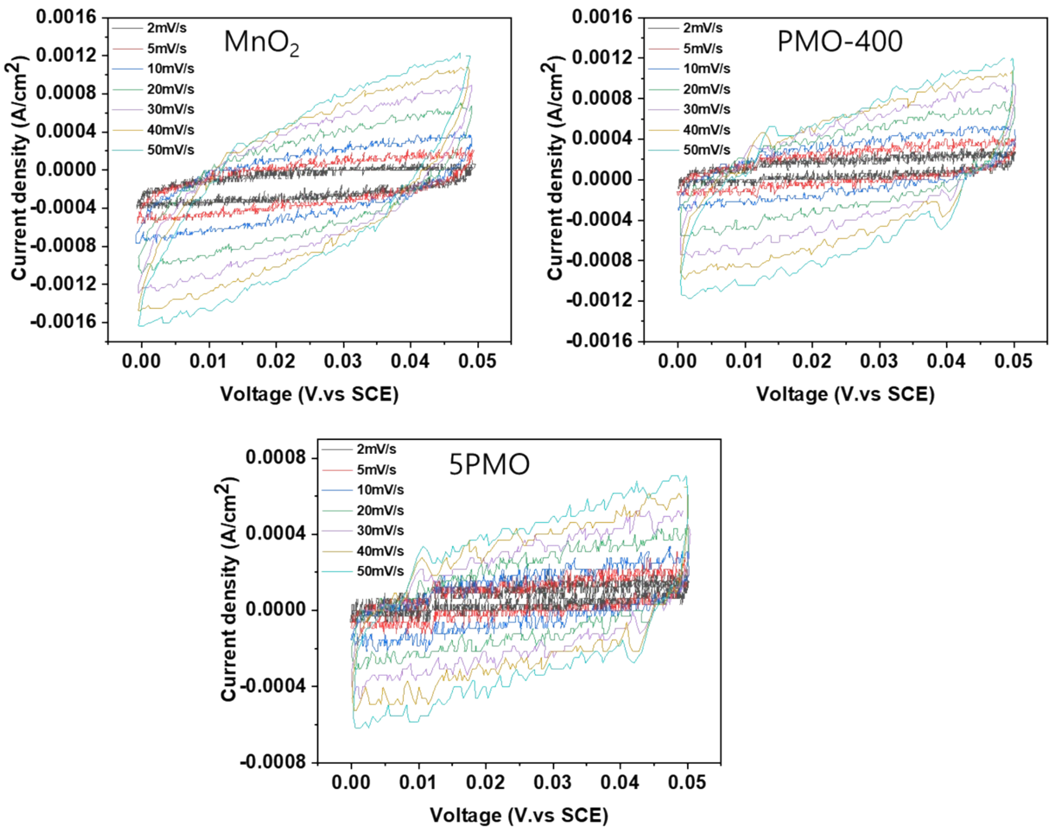

Figure S7. CV curves of MnO_2, PMO-400 and 5PMO electrodes at different scan rates.

Table S1. Electrochemical performance of 5PMO electrode compared with MnO_2-based systems.

Sl. No.	**Electrode material**	**Electrolyte**	**Specific capacitance (F/g)**	**Rate Capability (%)**	**Cycling Stability (at cycles)**	**Ref.**
1	P-Co_2MnO_{4-x}	3M KOH	838F/g at 1A/g	74.5% (1 to 10A/g)	80.3% at 10,000cycle	[1]
2	Cobalt Manganese Phosphate	1M KOH	571F/g at 2.2A/g		88% at 8,000 cycle (3A/g)	[2]
3	$Mn_{0.5}Co_{0.5}(HPO_4)$	3M KOH	1727F/g at 1A/g	77.3% (1 to 10A/g)		[3]
4	MnO_2-CNFs cable	1M Na_2SO_4	324.55F/g at 0.5A/g		62% at 100 cycle (1A/g)	[4]
5	MnO_2/nitrogen doped Carbon	1M Na_2SO_4	480.3F/g at 0.5mA/cm^2	70% (0.5 to 40A/cm^2)	97% at 10,000 cycle (0.5mA/cm^2)	[5]
6	Alpha-MnO_2	1M Na_2SO_4	235F/g at 1A/g	76.6% (0.5 to 10A/g)	95% at 3,000 cycle (3A/g)	[6]
7	MnO_2/Ant-nest like hierarchical porous carbon	6M KOH	662F/g at 1A/g	50.3% (1 to 10A/g)	-	[7]
8	Mn^{3+}/Mn^{4+} ratio controlled MnO_2 / CC	1M Na_2SO_4	408.1F/g at 1A/g	46% (1 to 16A/g)	99.4% at 2,000 cycle (10A/g)	[8]
9	PANI/Ag@MnO_2 nanorod	2M KOH	1028.66F/g at 1A/g	69.1% (1 to 20A/g)	91.3% at 5,000 cycle (10A/g)	[9]
10	5nm NiO ALD P-MnO_2	2M KOH	2294.78F/g at 5A/g	79.0% (5 to 20A/g)	85.8% at 20,000 cycle (20A/g)	This work

Table S2. Device performance of 5PMO//rGO device compared with MnO_2-based systems.

Sl. No.	Positive Electrode Material	Negative Electrode Material	Energy density (Wh/kg)	Power density (W/kg)	Cycling Stability (at cycles)	Ref.
1	P-Co_2MnO_{4-x}	Activated carbon	25.18	800.07	89.5% at 10,000 cycle	[1]
2	Cobalt Manganese Phosphate	rGO	45.7	1650	87% at 6,000 cycle (2.5A/g)	[2]
3	$Mn_{0.5}Co_{0.5}(HPO_4)$	G-ink	56.16	599.92	95.5% at 5,000 cycle (5A/g)	[3]
4	MnO_2-CNFs cable	MnO_2-CNFs cable	16.7	400		[4]
5	MnO_2/nitrogen doped Carbon	1T-MoS_2/Gr	3.62	18.7	90.1% at 10,000 cycle (10mV/s)	[5]
6	Alpha-MnO_2	Activated carbon	28.9	200	94% at 5,000 cycle (1A/g)	[6]
7	MnO_2/Ant-nest like hierarchical porous carbon	MnO_2/Ant-nest like hierarchical porous carbon	14.5	5000	93.4% at 5,000 cycle (1A/g)	[7]
8	Mn^{3+}/Mn^{4+} ratio controlled MnO_2 / CC	FeOOH/C	55.9	1240	-	[8]
9	PANI/Ag@MnO_2 nanorod	AC	49.66	1599.75	88.6% at 5,000 cycle (10A/g)	[9]
10	5nm NiO ALD P-MnO_2	rGO	71.975	1599	87.0% at 23,000 cycle (10A/g)	This work

References:

[1] K.-S. Ahn, R. Vinodh, B.G. Pollet, R.S. Babu, V. Ramkumar, S.-C. Kim, K. Krishnakumar, H.-J. Kim, A high-performance asymmetric supercapacitor consists of binder free electrode materials of bimetallic hydrogen phosphate (MnCo (HPO4)) hexagonal tubes and graphene ink, Electrochimica Acta, 426 (2022) 140763.

[2] S. Dang, Y. Wen, T. Qin, J. Hao, H. Li, J. Huang, D. Yan, G. Cao, S. Peng, Nanostructured manganese dioxide with adjustable Mn3+/Mn4+ ratio for flexible high-energy quasi-solid supercapacitors, Chemical Engineering Journal, 396 (2020) 125342.

[3] J.M. Jeong, S.H. Park, H.J. Park, S.B. Jin, S.G. Son, J.M. Moon, H. Suh, B.G. Choi, Alternative-Ultrathin Assembling of Exfoliated Manganese Dioxide and Nitrogen-Doped Carbon Layers for High-Mass-Loading Supercapacitors with Outstanding Capacitance and Impressive Rate Capability, Advanced Functional Materials, 31 (2021) 2009632.

[4] P.K. Katkar, S.J. Marje, V.G. Parale, C.D. Lokhande, J.L. Gunjakar, H.-H. Park, U.M. Patil, Fabrication of a high-performance hybrid supercapacitor based on hydrothermally synthesized highly stable cobalt manganese phosphate thin films, Langmuir, 37 (2021) 5260-5274.

[5] C.-S. Liu, C.-L. Huang, H.-C. Fang, K.-Y. Hung, C.-A. Su, Y.-Y. Li, MnO2-based carbon nanofiber cable for supercapacitor applications, Journal of Energy Storage, 33 (2021) 102130.

[6] Q. Lu, X. Wang, M. Chen, B. Lu, M. Liu, T. Xing, X. Wang, Manganese dioxide/ant-nest-like hierarchical porous carbon composite with robust supercapacitive performances, ACS Sustainable Chemistry & Engineering, 6 (2018) 7362-7371.

[7] M.B. Poudel, M. Shin, H.J. Kim, Polyaniline-silver-manganese dioxide nanorod ternary composite for asymmetric supercapacitor with remarkable electrochemical performance, International Journal of Hydrogen Energy, 46 (2021) 474-485.

[8] Z. Wang, J. Gu, S. Li, G.C. Zhang, J. Zhong, X. Fan, D. Yuan, S. Tang, D. Xiao, One-step polyoxometalates-assisted synthesis of manganese dioxide for asymmetric supercapacitors with enhanced cycling lifespan, ACS Sustainable Chemistry & Engineering, 7 (2018) 258-264.

[9] F. Xiang, X. Zhou, X. Yue, Q. Hu, Q. Zheng, D. Lin, An oxygen-deficient cobalt-manganese oxide nanowire doped with P designed for high performance asymmetric supercapacitor, Electrochimica Acta, 379 (2021) 138178.